NRC Publications Archive
Archives des publications du CNRC

Dynamic wetting spread factors and interfacial heat transfer coefficients in the solidification of aluminum droplets on copper substrates

Tremblay, David-Alexandre; Bouchard, Dominique; Kiss, Laszlo

This publication could be one of several versions: author's original, accepted manuscript or the publisher's version. / La version de cette publication peut être l'une des suivantes : la version prépublication de l'auteur, la version acceptée du manuscrit ou la version de l'éditeur.

Publisher's version / Version de l'éditeur:

Conference of Metallurgists (COM) 2005 [Proceedings], 2005-08-25

NRC Publications Archive Record / Notice des Archives des publications du CNRC :
https://nrc-publications.canada.ca/eng/view/object/?id=e4b44ba3-4126-4927-99d4-e8f5dd8b13b
https://publications-cnrc.canada.ca/fra/voir/objet/?id=e4b44ba3-4126-4927-99d4-e8f5dd8b13b8

Access and use of this website and the material on it are subject to the Terms and Conditions set forth at
https://nrc-publications.canada.ca/eng/copyright
READ THESE TERMS AND CONDITIONS CAREFULLY BEFORE USING THIS WEBSITE.

L'accès à ce site Web et l'utilisation de son contenu sont assujettis aux conditions présentées dans le site
https://publications-cnrc.canada.ca/fra/droits
LISEZ CES CONDITIONS ATTENTIVEMENT AVANT D'UTILISER CE SITE WEB.

Questions? Contact the NRC Publications Archive team at
PublicationsArchive-ArchivesPublications@nrc-cnrc.gc.ca. If you wish to email the authors directly, please see the first page of the publication for their contact information.

Vous avez des questions? Nous pouvons vous aider. Pour communiquer directement avec un auteur, consultez la première page de la revue dans laquelle son article a été publié afin de trouver ses coordonnées. Si vous n'arrivez pas à les repérer, communiquez avec nous à PublicationsArchive-ArchivesPublications@nrc-cnrc.gc.ca.

National Research Council Canada
Conseil national de recherches Canada

Dynamic wetting spread factors and interfacial heat transfer coefficients in the solidification of aluminum droplets on copper substrates

David-Alexandre Tremblay and Dominique Bouchard
Aluminium Technology Centre
501, Boul. Université, Chicoutimi
Québec, Canada, G7H 8C3

László Kiss
Université du Québec à Chicoutimi (UQAC)
555 Boul. Université, Chicoutimi,
Québec, Canada, G7H 2B1

ABSTRACT

Dynamic wetting spread factors and interfacial heat transfer coefficients were determined for aluminum droplets solidifying on copper substrates. The spread factors were determined from the droplet geometries while the heat transfer coefficients were obtained by solving inverse heat conduction problems. 1-D and 2-D heat transfer models are presented and the results they provided are compared. For the latter, a sensitivity analysis was also performed to determine the influence of thermophysical properties and boundary conditions. Experiments were alternatively carried out with three different gaseous atmospheres and the dynamic wetting spread factors were correlated to the interfacial heat transfer coefficients.

INTRODUCTION

Many defects develop at the initiation of solidification where dynamic wetting and heat transfer intervene. Understanding and controlling these two phenomena is thus instrumental in many processes involving liquid metals solidifying on metallic substrates, for example die casting (1,2), strip casting (3-5) and thermal spraying (6). Wetting defines the capacity of a liquid to spread on a given surface (7). Under non-equilibrium solidification conditions, it is a dynamic process that evolves over a short time scale. As dynamic wetting occurs, heat is also transferred from the solidifying metal to the substrate. The thermal resistance that develops at the interface between the metal and the substrate is in many cases the primary factor that dictates the cooling rate and this has repercussions on the mechanical properties of the solidified component.

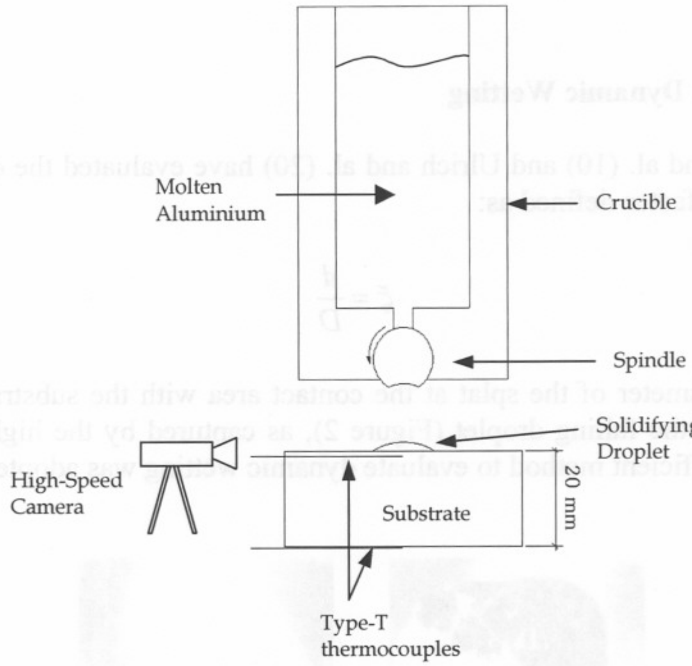

Figure 1 - Schematic of the Experimental Set-Up for the Simultaneous Characterization of Dynamic Wetting and Heat Transfer

Table 1 – Thermophysical Properties of ETP Copper and AA 1080 Aluminium

Property (Units)	Value	Ref.
ETP Copper		
Heat capacity ($kJ\ kg^{-1}\ K^{-1}$)	$4.77\cdot10^{-1}-1.68\cdot10^{-4}T-5.07\cdot10^{3}T^{-}$ $+1.49\cdot10^{-7}T^{2}$	16
Thermal Conductivity ($W\ m^{-1}\ K^{-1}$)	$419-6\cdot10^{-2}T$	17
Density ($kg\ m^{-3}$)	8960	18
Aluminium AA 1080		
Heat Capacity, Solid ($kJ\ kg^{-1}\ K^{-1}$)	$1.16-6.08\cdot10^{-4}T-1.33\cdot10^{4}T^{-2}$ $+7.69\cdot10^{-7}T^{2}$	16
Heat Capacity, Liquid ($kJ\ kg^{-1}\ K^{-1}$)	1.17	16
Thermal Conductivity, Solid ($W\ m^{-1}\ K^{-1}$)	$2.64\cdot10^{2}-5.63\cdot10^{-2}T$	17
Thermal Conductivity, Liquid ($W\ m^{-1}\ K^{-1}$)	$6.0\cdot10^{1}+3.27\cdot10^{-2}T$	17
Solidus Temperature (K)	919.15	19
Liquidus Temperature (K)	930.15	19
Density ($kg\ m^{-3}$)	2700	19
Latent Heat of Solidification ($kJ\ kg^{-1}$)	396.6	16

THEORY

Evaluation of the Dynamic Wetting

Amanda and al. (10) and Ulrich and al. (20) have evaluated the dynamic wetting using a spreading factor defined as:

$$\xi = \frac{d}{D} \tag{1}$$

where d is the diameter of the splat at the contact area with the substrate and D is the mean diameter of the falling droplet (Figure 2), as captured by the high speed camera. This simple and efficient method to evaluate dynamic wetting was adopted in this study.

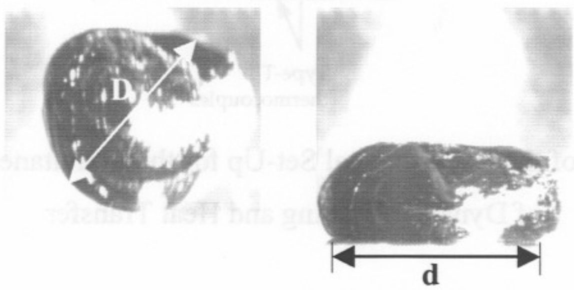

Figure 2 – Illustration of the Mean Diameter of the Falling Droplet, D, and Diameter of the Splat, d, Used for the Calculation of the Spreading Factor

Evaluation of the Interfacial Heat Transfer Coefficient

As the liquid metal droplet impinged the substrate, heat was transferred at the interface with the substrate. The transient heat flow at this interface can be described by Newton's law of cooling (21):

$$q(t) = h(t)(T_D^I(t) - T_S^I(t)) \tag{2}$$

In this study, the parameters in Equation 2 were determined in two distinct steps. The first involved solving a classical inverse heat-conduction problem (IHCP) to obtain the heat flux entering the substrate, *q(t)*. It was assumed that this flux did not vary along the radius of the splat. The sequential function specification method was used to determine the flux and details on its use have been given elsewhere (22). The second step involved solving two direct problems (one for the substrate and one for the droplet) to determine the temperature profiles in the substrate and the droplet. The interfacial temperatures of the droplet and the substrate, $T_D^I(t)$ and $T_S^I(t)$, were then extracted from these profiles and inserted with the heat flux, *q(t,)* in Equation (2) to obtain the interfacial heat transfer coefficient, *h(t)*.

The direct problem was solved using the heat conduction equation for unsteady states, expressed below for the substrate in 2-D Cartesian coordinates:

$$\frac{\partial}{\partial x}\left(k\frac{\partial T}{\partial x}\right)+\frac{\partial}{\partial y}\left(k\frac{\partial T}{\partial y}\right)=\rho C_p\frac{\partial T}{\partial t} \tag{3}$$

Explicit finite difference approximations of this equation were used to calculate the temperature evolution in the substrate. Some of the calculations in this work compared a 2-D with a 1-D formulation for the substrate. In the latter case, Equation (3) was simplified to account for a single coordinate. For the droplet, a 1-D model was used along with an enthalpy formulation (23) to account for solidification. The selection of the 1-D model for the droplet was based on the observation that the amount of heat transferred from the free surface of the splat was small compared to what is transferred at the interface with the substrate. This aspect is further discussed in the next section. Thermal energy transported by convection in the liquid pool of the droplet was also accounted with an effective thermal conductivity, k_{eff}, defined as (24).

$$k_{eff}=k_c * k(T) \qquad T\geq T_L \tag{4}$$

$$k_{eff}=f_s * k_s(T)+f_l * k_l(T) * \left[1+(k_c-1) * \left(\frac{T-T_S}{T_L-T_S}\right)^2\right] \qquad T_S\leq T\leq T_L \tag{5}$$

The value of k_c in those equations is typically between 5 and 10. The solid and liquid fractions, f_s and f_l, respectively, were calculated assuming they varied linearly with temperature. The boundary conditions of the substrate were fixed by imposing the heat flux, *q(t)* in Equation (2), at the substrate/droplet interface while all the other substrate boundaries were treated adiabatically. For the droplet, the heat flux, *q(t)*, was also used as a boundary condition for the interface with the substrate and the top surface was treated with heat flow by natural convection, (h = 15 W m^{-2} K^{-1}, (25)), and radiation, (emissivity = 0.17, (26)). The initial temperature of the substrate was given by its thermocouples and was typically 25 °C while the initial temperature for the droplet was 725 °C.

RESULTS AND DISCUSSION

In the experiments conducted in this study, the size of the droplet was small compared to that of the substrate. A consequence of that was that heat diffused in the substrate from top to bottom as well as laterally. A 1-D model only accounts for the top to bottom heat flow while a 2-D model accounts for top to bottom and lateral heat flows. The 2-D model should in principle provide more accurate results since it is a more complete description. To this effect, it is therefore interesting to compare differences in the solutions produced by the 1-D and 2-D models.

The first set of calculations was carried out by imposing adiabatic conditions at the back of the substrate. This was a fair assumption considering the respective sizes of the droplets and the substrates. The experiments required for these calculations were conducted with droplets falling in a gas phase composed of air. The results are shown in Figure 3 and it is observed that the 1-D model provides a lower interfacial heat flux than the 2-D model. This is consistent since a greater flux is required to account for the heat transferred laterally.

The area under these curves yields the total energy per unit area at the splat/substrate interface and in the 0.5 s time period shown in this Figure, it is approximately 35 % greater with the 2-D model. The lateral heat flow is therefore an important element of the process. Also shown in Figure 3 are grayscale illustrations of the substrate temperature fields that the two models yield at 100, 250 and 500 ms. In Figure 4, the heat transfer coefficients obtained with the 1-D and 2-D models are shown. It is seen that the values with the 1-D model are also lower than those obtained with the 2-D model.

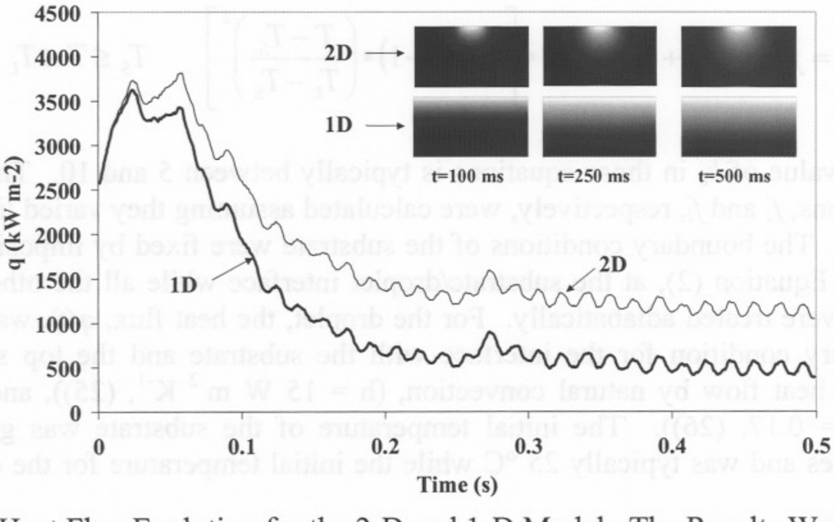

Figure 3 – Heat Flux Evolution for the 2-D and 1-D Model. The Results Were Obtained With Droplets Falling on the Substrate in a Gas Phase Composed of Air. Adiabatic Conditions Were Imposed at the Back of the 20 mm Thick Substrate in Both Models. The Grayscale Representations of the Temperature Fields Adjoining the Curves Illustrate the Differences in the Lateral Temperature Distributions Between the 1-D and 2-D Models.

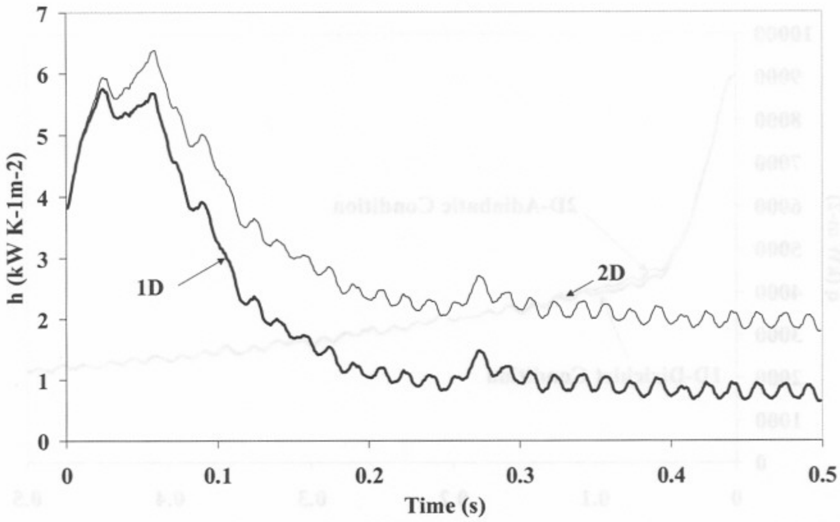

Figure 4 – Evolution of the Heat Transfer Coefficients Calculated With the Heat Fluxes in Figure 3

A different set of experiments and calculations were then carried out to evaluate the influence of the boundary condition at the back of the substrate. The 2-D model with the adiabatic condition used previously was compared to a 1-D model with a Dirichlet condition (23). The latter was obtained by placing a thermocouple 5 mm below the surface of the substrate. This thermocouple was in addition to the one normally placed 1 mm below the surface of the substrate used to characterize the boundary condition at the interface between the droplet and the substrate. In this version of the of the 1-D model, it was thus assumed that the substrate had a thickness of only 5 mm and the boundary condition at this location was given by the thermocouple at this location. This model was also used in a previous study (15).

The results are shown in Figure 5 and it is noted that the difference between this new 1-D model and the 2-D model is small. As mentioned earlier, the 1-D and 2-D models differ in that the latter accounts for lateral heat flow while the former does not. However, the results in Figure 5 suggest that this lateral flow is small over a thickness of 5 mm. A 1-D model can then be a good approximation of the heat flow, provided that a Dirichlet condition sufficiently close to the surface is supplied. The 2-D model remains advantageous in that it does not require this extra thermocouple. To this effect, it should be realized that thermocouples and the holes that need to be drilled for their insertion produce perturbations in the heat flow and uncertainties are affixed to the values they provide. There is thus an incentive to minimize their numbers. In Figure 6, the interfacial heat transfer coefficients associated to these two models are shown. It is seen that as for the heat fluxes, the values are close to one another.

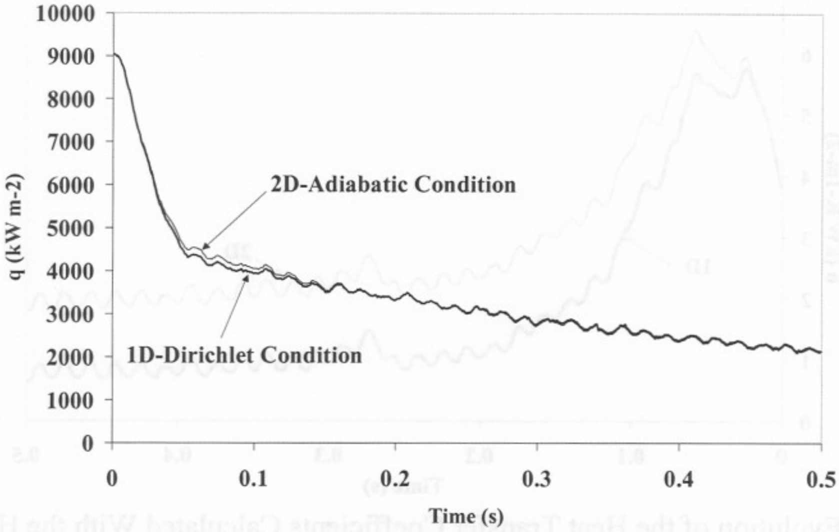

Figure 5 – Heat Flux Evolution for the 2-D and 1-D Models. An Adiabatic Condition Was Imposed at the Back of the Substrate for the 2-D Model While a Dirichlet Condition Was Used for the 1-D Model. With the Application of the Dirichlet Condition, the 1-D Model Provides Results in Close Agreement With the 2-D Model.

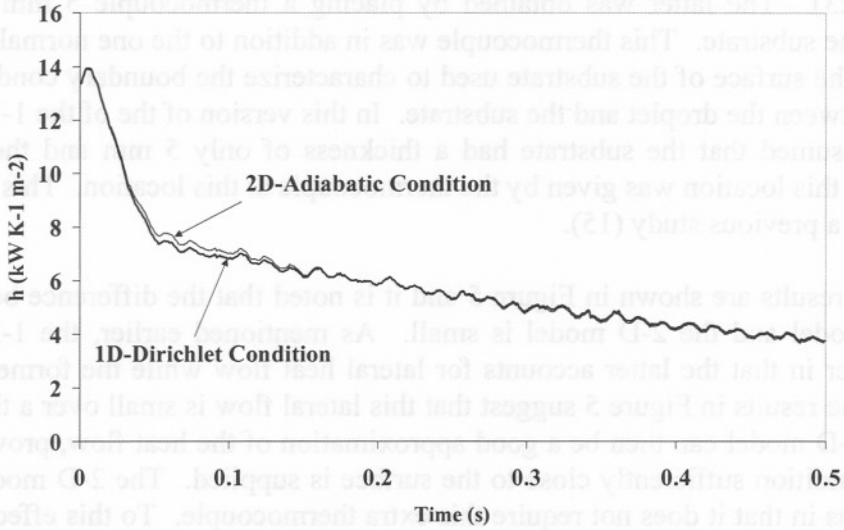

Figure 6 – Interfacial Heat Transfer Coefficients Calculated Using the Fluxes in Figure 5.

Other factors that may influence the calculated interfacial heat fluxes and heat transfer coefficients are heat flows by convection and radiation from the droplet to the surrounding gas phase. As mentioned earlier, these were accounted in the present work for the top surface of the droplet. In Figure 7, the evolution of the interfacial heat transfer coefficients when convection and radiation are accounted can be compared to the solution obtained when this is replaced by an adiabatic condition. It is seen that the contribution of convection and radiation on the calculated interfacial heat transfer coefficient is negligible.

Also shown in this Figure is the evolution of the temperature of the droplet at the interface with the substrate where a rebound is produced after approximately 0.1 s. This can be explained from the evolution of the interfacial heat transfer coefficient shown in the same Figure. Its very large initial value is indicative of the good thermal contact between the solidifying metal and the substrate and this produces a rapid temperature drop. The heat transfer coefficient however decreases rapidly and this is normally attributed to formation of a gap at the interface which produces a poor thermal contact between the droplet and the substrate (1). However, there is still metal that remains to be solidified in the liquid pool of the droplet and the heat this pool contains is conducted to the interface. Since the thermal contact with the substrate is poor, the heat is not transferred to the substrate as readily and the surface temperature of the droplet then increases.

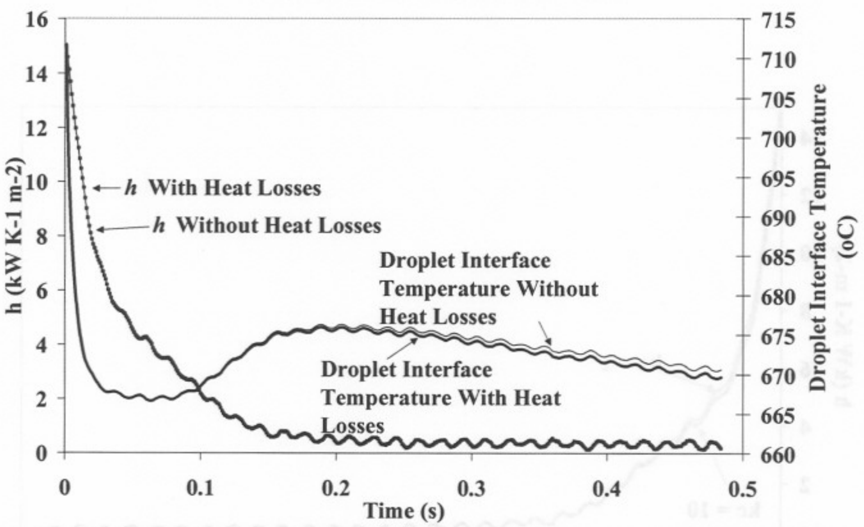

Figure 7 – Influence of Heat Losses by Convection and Radiation to the Surroundings on the Interfacial Heat Transfer Coefficients and the Interfacial Droplet Temperatures. The Curves that Account for the Heat Losses are Superimposed on those that Do Not Account for them Indicating the Losses are Negligible.

Another factor that may affect heat transfer during solidification is convection within the droplet. As shown in Figure 8, the droplet wiggles after impinging the substrate and this produces convection in the liquid pool of the droplet that may enhance the heat transfer. As described in the previous section, this convection may be accounted by using an effective thermal conductivity, as defined in Equations (4) and (5). Figure 9 illustrates the results obtained when the multiplying factors of this effective conductivity are varied in the typical range of 1 to 10. There is no significant difference in the values of the interfacial heat transfer coefficients and it thus appears that conduction is the main heat flow mechanism in the droplet.

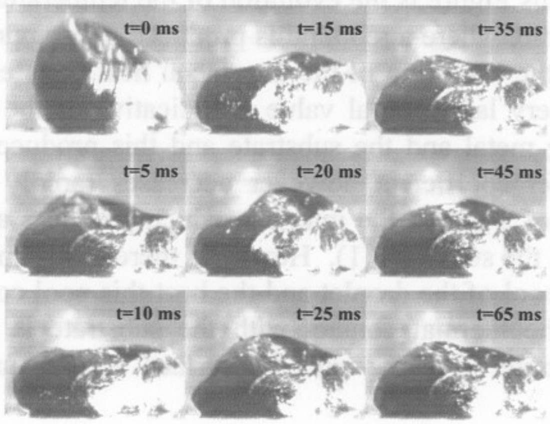

Figure 8 - Droplet Shape Evolution During Solidification. A Significant Movement of the Free Surface is Observed.

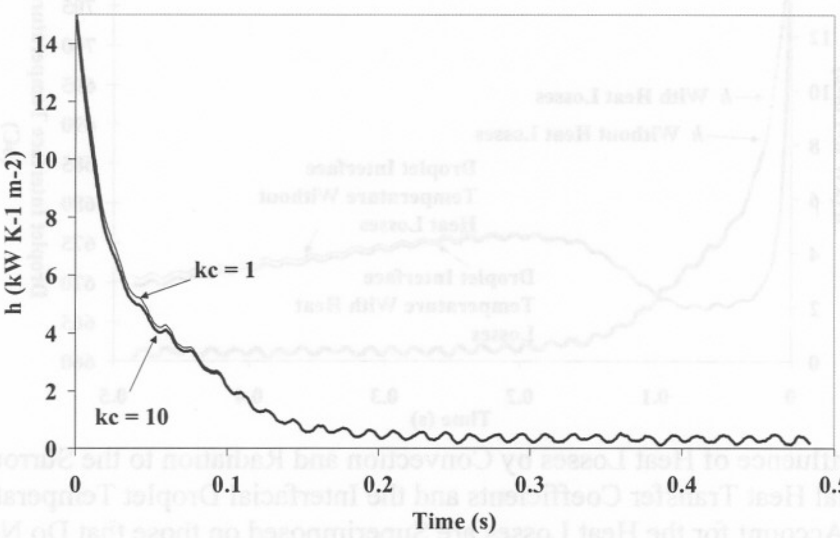

Figure 9 - Influence of the Multiplying Factor k_c Accounting for the Convection in the Droplet on the Calculation of the Interfacial Heat Transfer Coefficient

The results presented thus far have dealt with heat transfer models, their boundary conditions and their thermophysical properties. Experiments were also carried out to determine if dynamic wetting spread factors would correlate with interfacial heat transfer coefficients. The effect of surrounding gas phase was investigated for this purpose and tests were carried out alternatively with air, helium and argon. The interfacial heat transfer coefficients were obtained with a 2-D model for the substrate, having an adiabatic boundary at the back and a 1-D model for the droplet, also with an adiabatic condition at the free surface.

The results of this investigation are shown in Figure 10 where the spread factors, ξ, are shown in conjunction with the interfacial coefficients. It is noted that the order in the values for the spread factors is the same as the one for the heat transfer coefficient. In a previous research, Leboeuf reported a similar behavior with heat fluxes (15). In the presence of a gas, several factors may affect dynamic wetting and heat transfer of the solidifying droplet, for example, the formation of an oxide layer on the droplet and the thickness of this layer, a layer of gas entrapped between the droplet and the substrate, the thermal conductivity of the gases, surface tension of aluminum with these gases, etc. More research will be required to identify the mechanisms that influence dynamic wetting and heat transfer and to determine if high values of dynamic spread factors always correlate with high values of heat transfer coefficients.

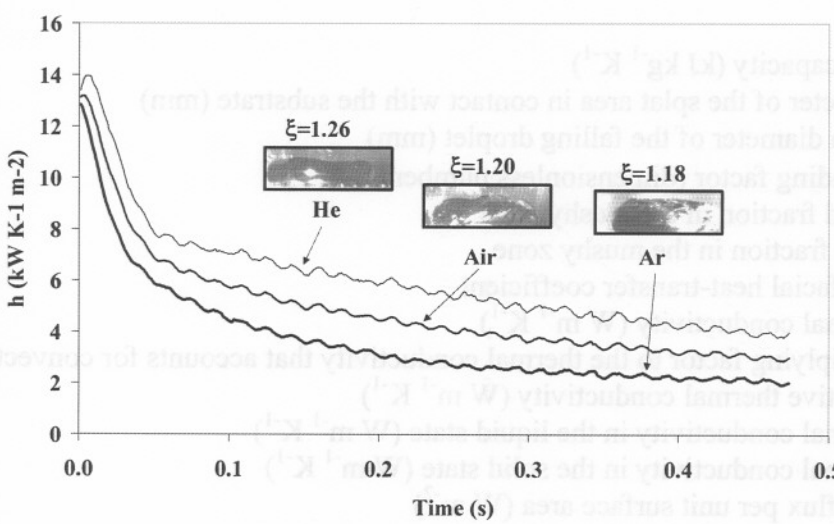

Figure 10 – Interfacial Heat Transfer Coefficients and Spread Factors Obtained in Three Different Atmospheres: Helium, Argon and Air. The Final Shapes of the Droplets are Also Shown.

CONCLUSIONS

A heat transfer analysis was performed for solidifying aluminum droplets on substrates. 2-D and 1-D models for the substrates were evaluated and it was observed that a 1-D model could produce results in very good agreement with the 2-D model when a Dirichlet boundary condition was imposed. The analysis performed on the droplet revealed that heat loss by convection and radiation to the surrounding gas had a negligible incidence on the calculated interfacial heat transfer coefficients. Thermal energy transported by convection in the liquid pool of the droplet was also found to be negligible. Solidification experiments carried out alternatively in the presence of air, helium and argon revealed a good correlation between the dynamic wetting spread factors and interfacial heat transfer coefficients.

ACKNOWLEDGEMENTS

Technical assistance from Martin Pruneau and Jean-Paul Nadeau, both with the Aluminum Technology Center and Sébastien Leboeuf, with the Arvida Research and Development Center, Alcan, Inc., is acknowledged. Discussions with Jinsoo Kim and Roderick I.L Guthrie from McGill University are also acknowledged.

NOMENCLATURE

C_p	heat capacity (kJ kg^{-1} K^{-1})
d	diameter of the splat area in contact with the substrate (mm)
D	mean diameter of the falling droplet (mm)
ξ	spreading factor (dimensionless number)
f_l	liquid fraction in the mushy zone
f_s	solid fraction in the mushy zone
h	interfacial heat-transfer coefficient
k	thermal conductivity (W m^{-1} K^{-1})
k_c	multiplying factor to the thermal conductivity that accounts for convection
k_{eff}	effective thermal conductivity (W m^{-1} K^{-1})
k_l	thermal conductivity in the liquid state (W m^{-1} K^{-1})
k_s	thermal conductivity in the solid state (W m^{-1} K^{-1})
q	heat flux per unit surface area (W m^{-2})
ρ	density (kg m^{-3})
t	time (s)
T	temperature (K)
T_D^I	interfacial temperature of the droplet (K)
T_L	liquidus temperature (K)
T_S	solidus temperature (K)
T_S^I	interfacial temperature of the substrate (K)

REFERENCES

1. C.P. Hallam and W.D. Griffiths, "A Model of the Interfacial Heat-Transfer Coefficient for the Aluminum Gravity Die-Casting Process," Metallurgical and Materials Transactions B, Vol. 35B, 2004, 721-733.

2. P. Schmidt, "Heat Transfer during Filling in Die Casting Processes," Materials Science and Engineering A, Vol. 173, 1993, 271-274.

3. L. Strezov, J. Herbertson and G. R. Belton, "Mechanisms of Initial Melt/Substrate Heat Transfer Pertinent to strip Casting," Metallurgical and Materials Transactions B, Vol. 31B, 2000, 1023-1030.

4. G. Li and B. G. Thomas, "Transient Thermal Model of the Continuous Single-Wheel Thin-Strip Casting Process," Metallurgical and Materials Transactions B, Vol. 27B, 1996, 509-525.

5. L. Strezov and J. Herbertson, "Experimental Studies of Interfacial Heat Transfer and Initial Solidification Pertinent to Strip Casting," ISIJ International, Vol. 38, No. 9, 1998, 959-966.

6. R. Asthana nad N. Sobczak "Wettability, Spreading, and Interfacial Phenomena in Hight- Temperature Coatings," JOM : the journal of the Minerals, Metals & Materials Society, Vol. 52, No. 1, 2000, pp. 18.

7. American Society of Metallurgy (ASM), Metals Handbook, Desk Edition, 1991

8. N. Ebrill, Y. Durandet and L. Strezov, "Dynamic Wetting and its Influence on Interfacial Resistance during Hot Dip Galvanizing," Trans. JWRI, Vol. 30, Special Issue, 2001, 351-359.

9. N. Ebrill, Y. Durandet and L. Strezov, "Dynamic Reactive Wetting and its Role in Hot Dip Coating of Steel Sheet with an Al-Zn-Si Alloy," Metallurgical and Materials Transactions B, Vol. 31B, 2000, 1069-1079.

10. S. Amanda, M. Haruyama, T. Ohyagi and K. Tomoyasu, "Wettability Effect on the Flattening Ratio of Molten Metal Droplets," Surface and Coating Technology, Vol. 138, 2001, 211-219.

11. T. Evans and L. Strezov, "Interfacial Heat Transfer and Nucleation of Steel on Metallic Substrates," Metallurgical and Materials Transactions B, Vol. 31B, October 2000, 1081-1089.

12. D. Bouchard, B. Howes, C. Paumelle, J.P. Nadeau, D. Simard and F.G. Hamel, "Control of Heat Transfer and Growth Uniformity of Solidifying Copper Shells through Substrate Temperature," Metallurgical and Materials Transactions B, Vol. 33B, June 2002, 403-411.

13. H. Todoroki, R. Lertarom, T. Suzuki and A.W. Cramb, "Heat Transfer Behavior of Pure Iron and Nickel against a Water Cooled Copper Mold During Initial Stage of Solidification," 1997 Ironmaking Conference Proceedings, 1997, 731-742.

14. G.X. Wang and E.F. Matthys, "Interfacial Thermal Contact during rapid solidification on a substrate," Heat Transfer 1994: Proceeding of the 10th International Heat Transfer Conference, Brighton, UK, 1994, 169-174.

15. S. Leboeuf, D. Bouchard, J.P. Nadeau, R.I.L. Guthrie and M. Isac, "Aluminium Droplets Impinging on a Copper Substrate: A Dynamic Wetting and Heat Transfer Study," Light Metals 2003: International Symposium on Light Metals as held at the 42nd Annual Conference of Metallurgists of CIM (COM 2003), Vancouver, Canada, 24-27 Aug. 2003, 215-227.

16. O. Kubaschewski, C. B. Alcock and P. J. Spencer, Materials Thermo-Chemistry, 6th Edition, Pergamon Press Ltd., New York, NY, USA, 1993, 274

17. Y. S. Touloukian, R.W. Powell, C. Y. Ho and P. G. Klemens, Thermophysical Properties of Matters, Vol. 1, Plenum Publishing Corp., New York, NY, USA, 1970, 81

18. E. A. Brandes and G. B. Brook, Smithells Metals Reference Book, 7th Edition, Butterworth-Heinemann, Oxford, United Kingdom, 1992, 14

19. MatWeb-Materials Property Database

20. J. Ulrich, M. Berg and K. Bauckhage, "Determination of a Splashing Threshold for Impacting Metal Droplets using High Speed Video Imaging," EPD Congress 1999 of The Minerals, Metals & Materials Society, 1999, 105-116

21. T.W. Clyne, "Modeling of Heat Flow in Solidification," Materials Science and Engineering, Vol. 65, 1984, 111-124

22. J. V Beck, "Nonlinear estimation applied to the nonlinear heat conduction problem." International Journal of Heat and Mass Transfer, Vol.13, No.4, 1970, 703-716

23. R. W. Lewis, P. Nithiarasu and K. N. Seetharamu, Fundamentals of Finite Element Method for Heat and Fluid Flow, John Wiley and Sons Ltd., Chichester, England, United Kingdom, 2004, 165.

24. B. Lally, L. Biegler and H. Henein, "Finite Difference Heat-Transfer Modeling for Continuous Casting," Metallurgical and Materials Transactions B, Vol. 21B, August 1990, 761-770

25. D. R. Gaskell, An Introduction to Transport Phenomena in Materials Engineering, Macmillan Publishing Company, New York, NY, USA, 1992

26. G. G. Gubareff, J.E. Janssen and R.H. Torborg, Thermal Radiation Properties Survey: a Review of the Literature, Honeywell Research Center, Minneapolis, MN, USA, 1960

Several studies on dynamic wetting (8-10) and heat transfer (11-14) have shown the crucial roles they play in solidification processes. These studies have however treated dynamic wetting and heat transfer as separate entities. In this work, a drop-splat set-up was used to simultaneously study dynamic wetting and heat transfer occurring in the solidification of aluminum. It is a follow-up of a previous work that examined the effect of selected experimental factors on wetting and heat transfer (15). In the previous study, dynamic wetting was characterized with spread factors while heat transfer was characterized with heat fluxes. The present study compares 1-D and 2-D heat transfer models and looks at the influence of boundary conditions and thermophysical properties on the results. Relationships between interfacial heat transfer coefficients and dynamic wetting spread factors obtained by conducting the drop-splat experiments in three different gaseous atmospheres are also presented.

EXPERIMENTAL

A depiction of the drop-splat set-up used for the experiments is given in Figure 1. It is similar to the ones constructed by Ebrill et al. (8, 9) and Leboeuf et al. (15). A resistance-heating element and a graphite crucible were used to melt commercially pure aluminum (AA 1080, 99.8%) to a temperature of 725°C. The graphite crucible had an approximate height of 155 mm and a diameter of 75 mm and 200 g of aluminum was typically melted. A graphite spindle in which a cavity was machined was fixed to the bottom of the crucible. During an experiment, an electric motor rotated the spindle, filling its cavity with molten aluminum and a droplet was released. Droplet volumes were determined by the size of the dimple machined in the spindle. Typically, droplet weights were in the range of 0.5 to 1.5 g to ensure that enough heat was transferred to the substrate. The substrates used were made of electrolytic tough pitched, ETP, copper (99.9+%) machined into 20 mm thick blocs having a width and length of 50 mm and 130 mm, respectively. The surface on which the droplets fell was polished to roughness of 0.15 μm R_a. This droplet impinged onto the substrate under free-fall conditions while a high-speed camera (Optikon, FastCam PCI) was used to film the sequence. A hole was drilled 1 mm below the surface of the substrate, parallel to the isotherms, in order to insert the type-T thermocouple that measured the temperature evolution of the substrate.

Images and temperatures were recorded simultaneously at a frequency of 1000 Hz. A moving table assured the proper alignment of the droplet with the thermocouple. A cooling system was fastened to the back of the substrate to cool the substrate between each experiment. Table 1 lists the thermophysical property data of the substrate and droplet materials utilized in the heat transfer calculations. The whole set-up was enclosed in an acrylic chamber to provide a controlled atmosphere and proper filming and lightning. Experiments were carried out alternatively with air (H_2O < 10 ppm, BOC Canada Ltd), helium (99.999%, Air Liquide Canada) and argon (99.998%, Air Liquide Canada).